Theory of the Thermodynamic Properties of Liquid Metals

Hilary D. Jones
Sandia Laboratories, Livermore, California 94550
(Received 24 October 1972)

Thermodynamic properties of the liquid metals Li, Na, K, and Al are calculated using a pseudopotential model together with an application of thermodynamic perturbation theory based on the Gibbs-Bogoliubov inequality. The theory is used to predict many properties associated with the melting phenomenon; for example, the melting temperature and density as a function of temperature, and the latent heat of fusion. It is found that the theory reproduces the trend in latent heats between the alkali metals, in contrast to previous work, although quantitative agreement with experiment is no better than has been obtained before. The theory is also applied to the prediction of thermodynamic properties on and away from the melting curve; in particular, the specific heat and velocity of sound of sodium are calculated over a wide range of temperature. Agreement with experiment is found to be good.

I. INTRODUCTION

The theoretical basis for a thorough understanding of the thermodynamics of simple insulating liquids (e.g., argon) has been forged in recent years to a point where it can be used to predict reliably the thermodynamic properties of real insulating materials.[1-4] This advance has been made possible in two ways. First, computer simulation makes it possible to conduct a controlled "experiment" on a well-defined system whose properties can be chosen to test the assumptions used in a proposed theory.[1,3] Computer simulations eliminate the uncertainty in the characterization of the experimental system so that one can assign any discrepancy between theory and "experiment" to some weakness in the theory and then make the necessary changes in the theory to extend its range of validity. Second, it has been determined how to expand the properties of liquids in a rapidly converging series, using the hard-sphere fluid as a zero-order approximation.[1,2,4] It has been possible to establish the reliability of such expansions only because the capability of doing computer simulation exists.

While numerous investigators have looked at simple insulating fluids, relatively few up to now have investigated the thermodynamics of liquid metals.[5-7] The situation is now changed with the recent wedding of pseudopotential theory to thermodynamic perturbation theory.[8,9] It is the object of this paper to elaborate on the work first presented by the author in Ref. 8, namely, the use of the theory to predict thermodynamic properties of a wide variety of liquid metals over a wide range of temperature and pressure. We will also have comments on the results of Stroud and Ashcroft[9] and Hartmann,[10] which are concerned with properties at the melting curve. In particular, we will demonstrate the usefulness of the theory in predicting the trend of the alkali-metal latent heats.

Traditionally, sodium has been the liquid metal most frequently considered because of its simple electronic structure, combined with the availability of experimental data (primarily at the melting point). However, it is now becoming possible to carry out equation-of-state measurements simultaneously at high pressure and temperature for a variety of metals,[11] and this should serve to stimulate interest in other metals, as well as in behavior away from the melting point and up towards the critical point, where the equation of state provides a probe of the band-structure changes associated with the metal-insulator (Mott) transition.[12]

Section II gives a brief review of pseudopotential theory as applied to liquid metals.[13] This will introduce the reader to the model used, and will demonstrate the fact that the "band-structure energy" of a metal is no more than a sum of pair potentials acting between ions. The resulting pair potential will be seen to be qualitatively correct even when the density is so low that the model is suspect. (Specifically, the pair potential provides reasonable estimates of the critical density and temperature.)

In Sec. III, a particular perturbation-theory technique is presented. It is based on the Gibbs-Bogoliubov inequality,[14] a theory which, while not the best available, is by far the most convenient to use. This approach has been tested primarily for the Lennard-Jones (LJ) pair potential, which differs from the metal potential in two important respects. First, the metal potential contains long-range Friedel oscillations while the LJ potential ostensibly has a short range. As will be shown, however, for *practical* purposes the metal potential has the shorter range of the two potentials.

The second difference is that the LJ potential has a steeper hard-core portion than does the metal potential. Since thermodynamic perturbation theory requires the metal potential approximate a hard-sphere potential, convergence of that theory becomes suspect. Recent computations by Hoover, *et al.* indicate that potential as soft as $1/r^4$ can be described by thermodynamic perturbation theory,[15] whereas, the metal potentials used here are at least as hard as $1/r^8$, so hard spheres should provide an adequate reference system.

In Sec. IV, we summarize the results of calculations for the alkali metals Li, Na, and K, as well as for aluminum. Thus, the melting curve is located; and the latent heat and volume change upon melting are determined, along with other properties associated with the melting phenomenon. The thermodynamic properties of the liquid phase are presented in the form of thermodynamic derivatives (compressibility, specific heat, thermal expansion, and so on). Particular emphasis is placed on the ability of the theory to reproduce trends between the alkali metals, in contrast to the previous work of Hartmann. To show the ability of the theory to predict thermodynamic properties away from the melting point, the specific heat is calculated over a wide range of temperatures. To show the limitations of the theory, the velocity of sound of sodium is calculated as a function of temperature and pressure.

II. MODEL PAIR POTENTIAL

Rather than repeating the well-known derivation[13] of a pair potential from pseudopotential theory, this section presents a very abbreviated sketch of the principles involved. This much should serve to introduce the notation used in the paper and to indicate the model pseudopotential being used.

Consider the energy of a conduction electron of wave vector $\vec{k}$ interacting with the potential set up by the ions. If there were no such interaction, the energy would be purely kinetic energy: $E_{\vec{k}} = \hbar^2 k^2/2m$; and the energy of all the electrons would then by $\sum_{\vec{k}} E_{\vec{k}}$, where the sum is carried up to the Fermi surface ($k < k_F$). (For the time being, exchange and correlation energies are neglected.) If one turns on a screened pseudopotential $W(r)$ to describe the spatial dependence of the electron-ion interaction, the conduction-electron energies will be changed. According to perturbation theory, the energy will become

$$E_{\vec{k}} = \frac{\hbar^2 k^2}{2m} + \langle \vec{k}|W(r)|\vec{k}\rangle + \sum_{\vec{q}\neq 0} \frac{\langle \vec{k}|W(r)|\vec{k}+\vec{q}\rangle\langle \vec{k}+\vec{q}|W(r)|\vec{k}\rangle}{(\hbar^2/2m)(k^2 - |\vec{k}+\vec{q}|^2)} + \cdots . \quad (1)$$

It is the last term of this equation that we are concerned with. If the pseudopotential can be separated into a sum of potentials localized at the ion positions $\vec{r}_i$[i.e., $W(r) = \sum_i w(\vec{r} - \vec{r}_i)$], then this contribution to the energy will have the form of a sum of pair potentials between ions i and j:

$$\sum_i \sum_j \left\{ \sum_{\vec{k}<k_F} \sum_{\vec{q}\neq 0} \frac{\langle \vec{k}|w(\vec{r}-\vec{r}_i)|\vec{k}+\vec{q}\rangle\langle \vec{k}+\vec{q}|w(\vec{r}-\vec{r}_j)|\vec{k}\rangle}{(\hbar^2/2m)[k^2 - |\vec{k}+\vec{q}|^2]} \right\}.$$

Since higher-order terms in Eq. (1) will involve higher powers of W, the terms will not always be reducible to a sum of pair potentials. Thus the validity of the pair-potential assumption for a metal is assured if the pseudopotential $w(r)$ is small. In what follows, this is assumed to be the case, not so much because it is true but because it is an assumption that is necessary to make a tractable theory. The successes of pseudopotential theory in other problems suggest that the approximation is valid.

Rather than pursue the derivation any further, thus repeating previous work,[13,16] the energy is written down in its final form. Thus,

$$E = E_{EG} + E_{BM} + E_{ES} + E_{BS} . \quad (2)$$

The term E_{EG} is the energy of the homogeneous electron gas,

$$E_{EG} = NZ[\tfrac{3}{5}\epsilon_F + \epsilon_X + \epsilon_C + w^{bc}(q=0)] . \quad (3)$$

Here, ϵ_F is the Fermi energy, ϵ_X and ϵ_C are the exchange and correlation energies, and $w^{bc}(q)$ is the (bare) core part of the pseudopotential.

The term E_{BM} is the energy contribution from the repulsive interaction between the core electrons on different ions, and it is taken to have the Born-Mayer form:

$$E_{BM} = \frac{1}{2}{\sum_{ij}}' \alpha e^{-\gamma r_{ij}} , \quad (4)$$

with α and γ as parameters, r_{ij} as the distance between ions i and j, and the sum restricted so that $i \neq j$.

The term E_{ES} is the electrostatic interaction energy of the ions, expressed as

$$E_{ES} = \frac{NZ^2e^2}{2}\left[\frac{4\pi}{\Omega}{\sum_{\vec{q}}}' \frac{S(q)S(-q)e^{(-q^2/4\mu^2)}}{q^2} + \frac{1}{N}{\sum_{ij}}' \frac{\operatorname{erfc}(\mu r_{ij})}{r_{ij}} - \left(\frac{2\mu}{\pi^{1/2}} + \frac{\pi}{\mu^2\Omega}\right)\right] . \quad (5)$$

Here Ω is the volume per ion, N is the number of ions, μ is a parameter chosen to make both sums converge rapidly, and $S(q)$ is the structure factor

$$S(q)=\frac{1}{N}\sum_i e^{i\vec{q}\cdot\vec{r}_i}. \tag{6}$$

The sum on q in Eq. (5) is restricted so that $q\neq 0$; thus the ions are in effect placed in a uniform negative-background charge.

Finally, E_{BS} is the band-structure energy, which is that part of Eq. (1) that depends on the ion positions. Thus

$$E_{BS}=N\sum_{\vec{q}}{}' S(q)S(-q)F(q), \tag{7}$$

where $F(q)$ is the energy wave-number characteristic. In the model used here, the screening of the electron gas has been modified to allow for exchange and correlation effects. The modification is that proposed by Geldart and Vosko,[17] and for $F(q)$ it leads to the form

$$F(q)=-\frac{\Omega q^2}{8\pi e^2}|w^b(q)|^2\frac{\epsilon(q)-1}{1+[\epsilon(q)-1)(1-g(q)]}, \tag{8}$$

where $\epsilon(q)$ is the Hartree dielectric constant, $w^b(q)$ is the bare pseudopotential, $g(q)$ is given by

$$g(q)=q^2/2(q^2+\xi k_F^2), \tag{9}$$

and ξ is determined by

$$\xi=0.916/(0.458+0.012r_s), \tag{10}$$

where r_s is given (in units of the Bohr radius) by $\frac{4}{3}\pi r_s^3=\Omega/Z$. Equation (10) assumes the Nozieres-Pines interpolation formula for the correlation energy, whence

$$\epsilon_x+\epsilon_c=-0.916/r_s-0.115+0.031\ln r_s.$$

Harrison's modified point-ion-model pseudopotential[13] has been used in the calculation,

$$w^b(q)=4\pi Ze^2/\Omega q^2+\beta/\Omega(1+q^2r_c^2)^2. \tag{11}$$

This model has the advantage that it converges rapidly to its asymptotic form at large q. Moreover, there are at our disposal two parameters, β and r_c, which represent the strength and range of the pseudopotential; thus we do not need to adjust separately the Hartree energy to give the proper lattice constant, as must be done with other potentials.[18] Note that this does not represent an increase in the number of parameters over the "single-parameter" Ashcroft pseudopotential, since for that potential the Hartree energy is frequently treated as a separate adjustable parameter.

It is desirable to rewrite the energy expression explicitly as a sum of pair potentials. To this end, consider the limit $\eta\to\infty$. If the expression for $S(q)$ from Eq. (6) is put into Eqs. (5) and (7), then these equations involve a sum on i and j, which includes terms where $i=j$. Also, in Eqs. (5) and (7), $q=0$ is excluded from the sum on q. If these equations are rewritten so that the $i=j$ term is separated out, and the $q=0$ term is restored, then the equations give

$$E_{ES}+E_{BS}=\frac{1}{2N}\sum_{\vec{q}}{}'\sum_{ij}{}'\left(\frac{4\pi Z^2e^2}{\Omega q^2}e^{-q^2/4\eta^2}+2F(q)\right)e^{i\vec{q}\cdot\vec{r}_{ij}}+\sum_{\vec{q}}F(q)$$
$$-\frac{1}{2N^2}\sum_{ij}\lim_{q\to 0}\left[e^{i\vec{q}\cdot\vec{r}_{ij}}\left(\frac{4\pi Z^2e^2}{\Omega q^2}e^{-q^2/4\eta^2}+2F(q)\right)\right]+\left(\frac{1}{2}\sum_{\vec{q}}\frac{4\pi Z^2e^2}{\Omega q^2}e^{-q^2/4\eta^2}-\frac{NZ^2e^2\eta}{\pi^{1/2}}\right).$$

The last term is identically zero, while the other terms are well behaved in the limit $\eta\to\infty$. This result combined with the previous equations gives a final expression for the energy

$$E=E_0+\frac{1}{2}\sum_{ij}{}'\phi(r_{ij}), \tag{12}$$

where

$$E_0=E_{EG}+\sum_{\vec{q}}F(q)-\frac{N}{2}\lim_{q\to 0}\psi(q), \tag{13}$$

$$\phi(r)=\alpha e^{-\gamma r}+\frac{1}{N}\sum_{\vec{q}}e^{i\vec{q}\cdot\vec{r}}\psi(q), \tag{14}$$

and $\psi(q)$ is defined as

$$\psi(q)=4\pi z^2e^2/\Omega q^2+2F(q). \tag{15}$$

It might appear that the $q=0$ term of Eq. (14) can be left out, since it is a correction to $\phi(r)$ of order $1/N$. To be consistent then, one would also have to remove the term $\lim_{q\to 0}\psi(q)$ from Eq. (13). However, the $q=0$ contribution to $\phi(r)$ is independent of r; so when $\phi(r_i-r_j)$ is summed over the N^2 pairs of atoms, the contribution to the energy is not negligible. In fact, the term in $\lim_{q\to 0}\psi(q)$ in Eq. (13) is necessary in order to get agreement between the energy calculated by Eqs. (12) and (2).[19]

The model presented above depends on four parameters: β, r_c, α, and γ. (Only the first two of these have an appreciable effect on thermodynamic properties.) For the alkali metals, the parameters were determined by Wallace in such a way to give a good fit to the lattice constant,

TABLE I. Parameters for the modified point-ion pseudopotential (β, r_c) and for the Born-Mayer potential (α, γ). Wallace's parameters for aluminum are shown in parentheses. The Bohr radius a_0 is used as the unit of length, and Rydbergs are the energy unit.

Metal	α (Ry)	γ (a_0^{-1})	β (Ry a_0^3)	$r_c(a_0)$
Li	0	0	23	0.33
Na	10.5	1.56	37	0.50
K	124	1.56	66	0.69
Al	0	0	42.9 (47.5)	0.29 (0.24)

internal energy, compressibility, and mean-square phonon frequency at zero temperature.[16] The values are given in Table I. For aluminum, Wallace chose to fit the parameters entirely to the phonon spectrum.[20] While this leads to an excellent fit of the phonon spectrum, it also leads to an unrealistic pseudopotential for most other calculations. In particular, it leads to a zero temperature density some $2\frac{1}{2}$ times too large. Put another way, the pressure required to sustain the lattice at the correct density would be −710 kbar; and the compressibility would then be negative. Clearly such unphysical results cannot be tolerated in an equation-of-state calculation. We have, therefore, refitted the pseudopotential parameters in the same manner as Wallace did the alkali metals. The results are shown in Table I, with Wallace's original values shown in parentheses for comparison. A preliminary calculation of the phonon spectrum using the new parameters still gives acceptable (7%) agreement with experiment, and the parameters now reduce the error in the density and other fitted quantities to only 7%.

Figure 1 shows the pair potential of sodium at melt density. (The other alkalis show qualitatively similar behavior, differing primarily only in the scales on the axes.) Plotted for comparison is a Lennard-Jones (LJ) potential chosen to fit the pair potential well. It will be seen that it has a much harder repulsive core than the actual potential. Moreover, despite the Friedel oscillations in the actual potential, the LJ potential is initially of longer range. It would be very difficult to assess which potential is the "longer ranged" from the practical standpoint of an equation-of-state calculation away from the critical point. Similar conclusions hold for the other alkali metals and aluminum.

Figure 2 shows the pair potential of aluminum at melt density. The potential differs qualitatively from that of Wallace[21] in the degree of structure in the potential well. However, the well depth, repulsive core, and Friedel oscillations are quantitatively similar to those of Wallace's potential.

Figure 3 shows the density dependence of $\phi(r)$

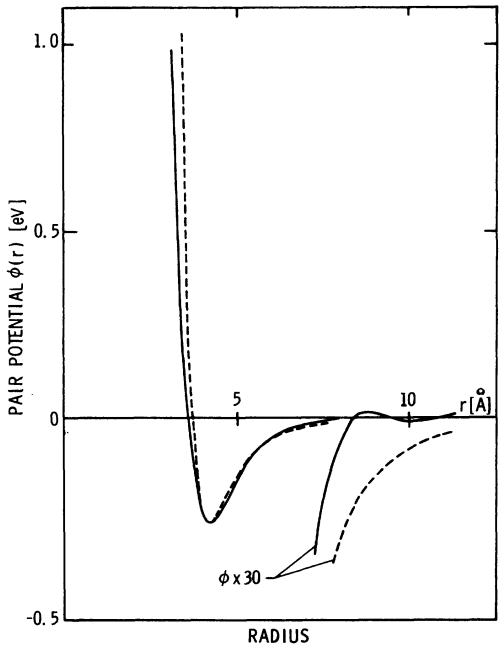

FIG. 1. Pair potential for sodium at the melt density (solid line). Broken line shows a Lennard-Jones potential for comparison. The scale is expanded by a factor of 30 at large r to show details of the Friedel oscillations.

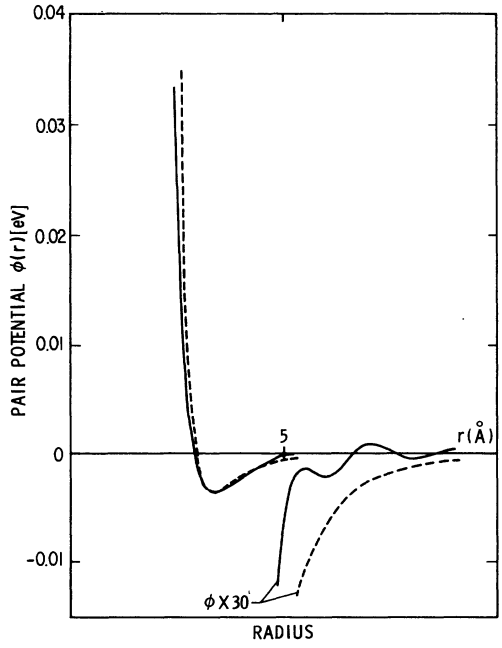

FIG. 2. Pair potential for aluminum at the melt density (solid line). Broken line shows the LJ potential for comparison.

for aluminum. (By contrast, the density dependence of the alkali metals is relatively weak, although at the critical density, the potential well is still some six times deeper than at normal density.) Figure 3 presents $\phi(r)$ at densities down to the estimated[22] critical density of aluminum, although at such densities, the model used becomes suspect.

There is an interesting consequence of such strong density dependence in $\phi(r)$. At normal liquid densities, the well depth corresponds to a temperature of $T = 336$ K. This would seem to indicate that a temperature on the order of 300 K would be sufficient to break the bonds between the atoms and to cause vaporization. But in fact, the critical temperature of aluminum is of order of 7000 K. This can be explained by the strong density dependence of the potential, since the density approaches the critical density, the well depth increases by an order of magnitude.

One can get a rough estimate of the critical density and temperature by means of the following argument. For a system with an LJ potential, it has been found[23] that the critical density ρ_c and temperature T_c are related to the repulsive core diameter σ and the potential well depth ϵ as follows:

$$\rho_c\sigma^3 = 0.36 \quad \text{and} \quad kT_c = 1.36\epsilon\,. \tag{16}$$

If it is assumed that these relations hold true for the metal potentials used here, then ρ_c and T_c can be estimated[24] (Table II). The experimental values of ρ_c and T_c are actually extrapolations of experimental data.[22]

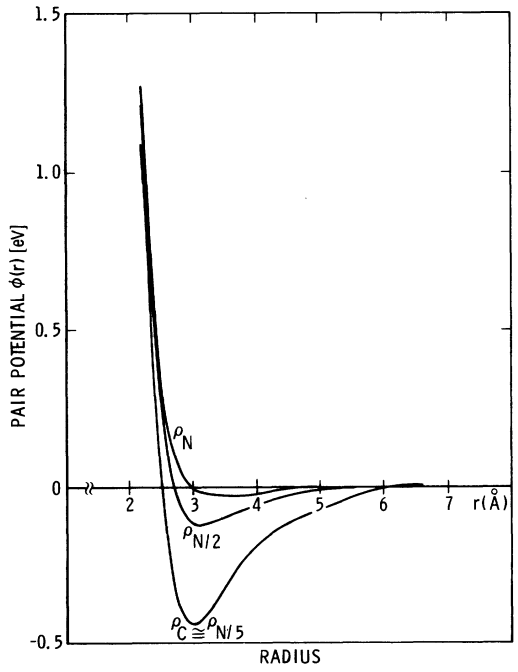

FIG. 3. Density dependence of the pair potential of aluminum. ρ_C is the estimated critical density, and ρ_N is the normal solid density.

The estimated critical temperatures agree reasonably well with experimental values, but the critical densities are too large by a factor of 2. Considering the crudeness of the approximations and the sensitivity of ρ_c to small changes in σ, the agreement with experiment can be considered good; and it demonstrates that, at least in a qualitative way, the density dependence of $\phi(r)$ is reasonable, even as one approaches the vicinity of the critical density where the theory must fail because of the metal-insulator transition. Further on, experimental evidence will be reviewed to show how far the theory can be carried toward the critical point.

III. FREE-ENERGY CALCULATION

The pair-potential model of a metal allows us to determine the free energy of the solid or liquid. When this is done, the melting curve can be determined by means of the requirement that the (Gibbs) free energies of the two phases be equal on the melting curve. Various temperature and/or volume derivatives of the free energy then allow a determination of the equation of state of the liquid or solid.

The calculation is not an easy one to do accurately, however. To get an idea of the problem, consider that the internal energies of the liquid and solid along the melting curve typically differ by only one part in 200; thus the small structural differences in the liquid and solid must be well characterized.

To calculate the free energy, a variational method based on the Gibbs-Bogoliubov inequality is used. The details of this calculation are given elsewhere[4,8,9] and will not be repeated here in detail. The method can be summarized as follows: One chooses a reference system which approximates the structure of the metal in the phase of

TABLE II. Critical constants of several metals based on the pair-potential characteristics. "Experimental" estimates are shown in parentheses and are really only estimates obtained by extrapolating experimental data. The term ρ_N is the normal solid density.

Metal	ρ_c/ρ_N	T_c (K)
Li	0.38 (0.20 ± 0.06)	2320 (3223 ± 600)
Na	0.42 (0.19 ± 0.05)	2250 (2573 ± 350)
K	0.44 (0.21 ± 0.04)	1920 (2223 ± 330)
Al	0.38	6900 (8000 ± 1500)

interest. Let the energy of the reference system be denoted E_R, with R some parameter characterizing the reference system. The energy E of the actual metal is given by Eq. (12). Then the Helmholtz free energy A of the metal is bounded above by

$$A \leq A_R + \langle E - E_R \rangle_R , \tag{17}$$

where A_R is the free energy of the reference system, and the expectation value takes $e^{-\beta E_R}$ as a weighting function ($\beta = 1/kT$). The inequality holds for all values of the parameter R; hence we can choose R so that the free energy is minimized.

For the solid, the Einstein model was used to define the reference system (each atom oscillates independently in a *harmonic* potential well). Thus R is the Einstein temperature θ. For the liquid, a hard-sphere reference system can be used, in which case R is the hard-sphere diameter σ. This choice of reference systems is essentially equivalent to Stroud and Ashcroft's choice,[9] once the high-temperature limit of their Debye-model reference system is recognized to be nothing but a form of Einstein model. However, the approximations used by them may destroy the validity of the inequality in Eq. (17).

In the pair-potential model, Eq. (17) can be rewritten as

$$A \leq A_R + E_0 - \langle E_R \rangle_R + \tfrac{1}{2}\rho \int d^3r\, g_R(r)\phi(r) , \tag{18}$$

where $g_R(r)$ is the radial distribution function of the reference system. In the case where $\phi(r)$ is the Fourier transform of $\psi(q)$ [Eq. (14) with the Born-Mayer term neglected], Eq. (18) may be rewritten as

$$A \leq A_R + E_0 + \tfrac{1}{2}\lim_{q\to 0}\psi(q) - \langle E_R \rangle_R + \frac{1}{2\rho}\int \frac{d^3q}{(2\pi)^3}\,\psi(q)[S_R(q) - 1] , \tag{19}$$

where $S_R(q)$ is the reference-system structure factor.

For the Einstein model, the structure factor is known exactly.[25] For the hard-sphere model, the Percus-Yevick equation structure factor was used for most of the calculations. Verlet and Weis[3] have suggested for this structure factor an empirical modification that agrees better with machine experiments. This modification has been considered also, but only to a limited extent, for it increases computation time by a factor of 2. Verlet and Weis give $g_\sigma(r)$ rather than $S_\sigma(q)$, but their expression can be Fourier-transformed analytically (the formula is too complicated to give here). Thus the Fourier-transform approach, Eq. (19), can still be used.

As mentioned elsewhere,[8] it is desirable to subtract out the large-q behavior of the integral in Eq. (19). This procedure requires that we be able to evaluate $\int d^3q\, q^{-2}[S_R(q) - 1]$ analytically. The result for the hard-sphere structure factor is given in Ref. 8. For the Einstein model, the integral can be evaluated in two ways: first, directly as an integral over q, which leads to

$$\int \frac{d^3q[S(q) - 1]}{q^2} = -4\pi^{3/2}\lambda + (2\pi)^3\rho \sum_{\vec{Q}}{}' \frac{e^{-Q^2/4\lambda^2}}{Q^2} , \tag{20}$$

where $\lambda = (Mk\theta^2/3\hbar^2T)^{1/2}$ and the sum is over the reciprocal lattice; or, second, the sum may be evaluated indirectly by observing the similarity of the sum in Eq. (20) to a sum needed to find the electrostatic energy of a metal. Thus if one uses an equality derived by Fuchs,[26] Eq. (20) can be transformed to read

$$\int \frac{d^3q[S(q) - 1]}{q^2} = \frac{2\pi\alpha'}{(3\Omega/4\pi)^{1/3}} + \frac{2\pi^3}{\Omega\lambda} - 2\pi^2 \sum_{\vec{\delta}}{}' \frac{\operatorname{erfc}\lambda\delta}{\delta} , \tag{21}$$

where erfc is the complementary error function, the sum is to be carried over the lattice, and $\alpha' = (-1.791\,72,\ -1.791\,68)$ for the (fcc, bcc) lattice. The sum in Eq. (21) converges more rapidly than that in Eq. (20) for the values of θ normally encountered.

The free energies of the Einstein model and hard-sphere model are as follows:

$$A_\theta - \langle E_\theta \rangle_\theta = NkT[\ln(\Lambda^3/v_F)] - \tfrac{3}{2}NkT \tag{22}$$

and

$$A_\sigma - \langle E_\sigma \rangle_\sigma = A_\sigma = A_{\text{id}} + NkT \times \left(-(a+1)\ln(1-\eta) + \frac{2a}{\eta - 1} + \frac{a+3}{2(\eta-1)^2} + \frac{3(a-1)}{2}\right) . \tag{23}$$

where $\Lambda = 2\pi\hbar/(2\pi MkT)^{1/2}$, $v_F = (2\pi\hbar^2T/Mk\Theta^2)^{3/2}$ (the free volume), $\eta = \frac{1}{6}\pi\rho\sigma^3$ (the packing fraction), and A_{id} is the ideal-gas free energy.

The constant a is determined as follows. Equation (23) is derived from the volume integral of the hard-sphere gas pressure. The pressure can be obtained in several ways: first, by the Virial theorem, which expresses the pressure as an integral of $\partial\phi/\partial r$ weighted by $g_\sigma(r)$, and second, by the Ornstein-Zernike theorem, which relates the compressibility to the integral of $g_\sigma(r) - 1$. If we assume the Percus-Yevick radial distribu-

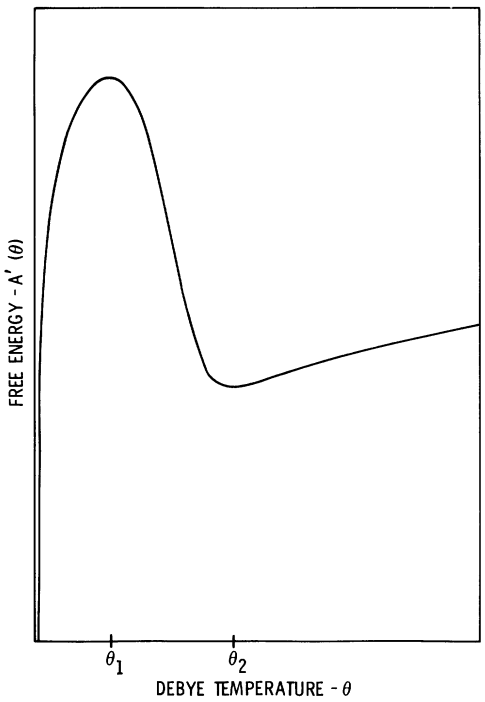

FIG. 4. Schematic dependence of the free-energy bounding function $A'(\theta)$ on the Einstein temperature θ.

tion function, these two approximations give the free energy if we set $a=-3$ and $a=0$, respectively. A third, and by far the best, way to determine a is to use the empirically determined Carnahan-Starling equation of state,[27] which leads to a value $a=-1$. Except where these approximations are explicitly tested, all calculations are carried out using the Percus-Yevick radial distribution function and the Carnahan-Starling approximation.

There is an anomaly of the Einstein model that needs to be pointed out. If one proceeds incautiously and uses Eq. (22) at small θ, it turns out that $A_\theta \to -\infty$ as $\theta \to 0$. Since $\langle E - E_\theta \rangle_\theta$ is bounded as $\theta \to 0$, Eq. (17) implies a negative infinite value for the free energy of the solid. The paradox is resolved because Eq. (22) holds only if θ is so large that the ions are localized to their lattice sites. If θ becomes so small that ions can exchange lattice sites, we must decide how to treat the reference-system internal energy U_0 for this configuration. It turns out that the simplest solution to this problem is to modify the reference-system potential so that it becomes infinite when two ions occupy the same cell. This has the effect of limiting the free volume of the cell surrounding a lattice site, and thereby eliminates the divergence.

This anomaly is illustrated further by Fig. 4, which plots the right-hand side of Eq. (17) [denoted $A'(\theta)$] as a function of θ. At both large and small θ, $A'(\theta)$ behaves as $kT \ln\theta$ and thus produces a divergence at small θ. It is clear that the "correct" bound to the free energy is $A(\theta_2)$. However, at very large temperatures, the $kT \ln\theta$ behavior dominates $A'(\theta)$, so that the region between θ_1 and θ_2 is only an inflection in $A'(\theta)$ (no minimum occurs). Stroud and Ashcroft interpret the temperature where $\theta_1 = \theta_2$ as an onset of mechanical instability, when in fact it appears to be merely a sign that the Einstein model is not being handled correctly (and, indeed, probably does not apply at all). The same "instability" noted by Choquard[28] occurs in self-consistent phonon theory. Fortunately, the effect occurs only at extremely high temperatures (~6000 °K) and has no relevance to ordinary calculations. (An obvious exception to this statement, of course, occurs with helium.)

IV. RESULTS

The calculations were refined to a high degree of accuracy in order that not only the free energy itself, but also the difference between the solid and liquid free energies will be free of numerical error. To achieve this goal, all integrals were evaluated by means of a Gauss-Legendre quadrature scheme. 30 points were used in each of several intervals, with the intervals refined near $q=2k_F$, where the dielectric constant is singular. In the evaluation of the solid free energy, reciprocal-lattice sums were carried out over 100 shells and were approximated by integrals beyond that

TABLE III. Melting properties of several metals. Experimental results are in parentheses. The theoretical results assume the hard-sphere liquid has $g_\sigma(r)$ given by the Percus-Yevick equation, and A_σ derived from the Carnahan-Starling approximation. The letter L is the latent heat of melting.

Metal	T_M (K)	V_s(cm^3/g)	$\Delta V/V_s$	L (cal/g)	$\partial T_M/\partial p$ (K/kbar)
Li	438 (452)	1.90 (1.93)	0.050 (0.015)	162 (103)	6.26 (3.03)
Na	346 (371)	1.06 (1.08)	0.048 (0.025)	40 (27)	10.8 (8.82)
K	318 (337)	1.20 (1.21)	0.048 (0.024)	21 (14.3)	20.3 (16.4)
Al	1170 (933)	0.40 (0.42)	0.046 (0.066)	109 (96)	4.78 (6.44)

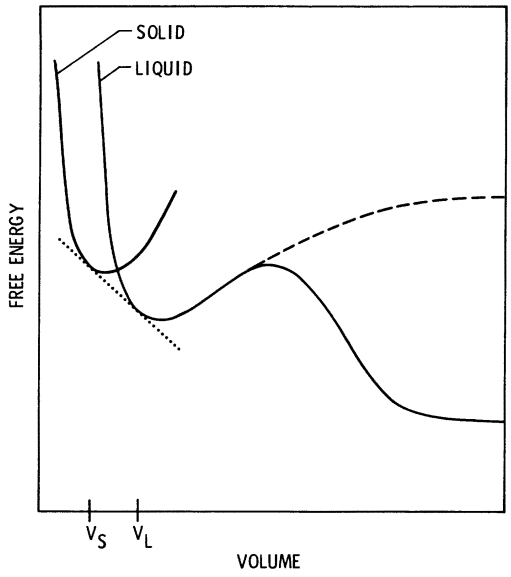

FIG. 5. Schematic dependence of the free energy on the volume for some fixed temperature. The dotted line is used to define the solid (V_S) and liquid (V_L) volumes at which melting occurs. The slope of the line determines the melting pressure at the given temperature. The dashed line shows the results of the theory, while the solid line is the proper behavior.

point. The calculation accuracy is such that a 10% change in the mesh size of the integration changes the free energies by only 1 part in 10^7, and the latent heat by 3 parts in 10^6. Similar changes occur when the sum on reciprocal-lattice vectors is extended. When the free energy is minimized with respect to σ or θ, the minimum is located to a degree of accuracy at least as good as 1 part in 10^8 in the free energy.

While such accuracy may seem inappropriate, it is in fact required if one is to locate the melting point or evaluated high-order derivatives of the free energy using finite differences. (For example, the temperature derivative of the velocity of sound is a third derivative of the free energy.) Moreover, the Gauss-Legendre quadrature is so efficient that high accuracy is not at all difficult to achieve.

Table III shows a number of properties of several metals associated with their melting (e.g., the melt temperature and density, latent heat of melting, volume change upon melting, and so on). These values are computed by calculating the free energies of the liquid and solid as functions of volume and temperature, then locating for each temperature the common tangent to the liquid and solid free-energy curves, as illustrated in Fig. 5.

The tangent points V_S and V_L give the solid and liquid volumes, while the slope of the line is the negative of the pressure required to have the solid melt at the given temperature. If one adjusts the temperature until the pressure is zero, the melting temperature and density can be found.

Table III shows the predicted melting properties of several metals along with the experimentally observed values. As found by Stroud and Ashcroft, agreement with experiment is on the whole satisfactory considering the problems inherent in this type of calculation. Moreover, we do reproduce the trend in the alkali-metal latent heats, in contrast to Hartmann's results.[10]

The source of the quantitative disagreement between theory and experiments, as is well known, is the fact that the free energies of liquid and solid are very nearly equal, so that small errors in the free energy cause large errors in the latent heat. We believe this to be the primary reason Hartmann failed to get the proper trend between the alkali-metal latent heats. To demonstrate this, consider the following expression for the internal energy of the liquid:

$$U \cong U_0 + \tfrac{1}{2}\rho \int g_\sigma(r)\phi(r)\, d^3r\,, \tag{24}$$

where U_0 is independent of σ.

For a hard-sphere system, $g_\sigma(r)$ may be very

TABLE IV. Model dependence of properties of liquid sodium near the melting point ($P = 0$). The models are: PY (Percus-Yevick), VW (Verlet-Weis), V (Virial theorem), CS (Carnahan-Starling), and OZ (Ornstein-Zernike). A, S, and L are the free energy, entropy, and latent heat. dp/dT is the slope of the melting curve.

Model $g_0(r)$	Model A_0	T_m (K)	ρ_{liq} (g/cm^3)	$\Delta V/V_{sol}$	A (cal/g)	S (cal/g-K)	L (cal/g)	dp/dT (kbar/K)
PY	V	270	0.933	0.027	−6529	0.5390	22	0.121
PY	CS	346	0.901	0.048	−6566	0.6366	40	0.093
PY	OZ	372	0.890	0.056	−6581	0.6650	45	0.085
VW	CS	395	0.879	0.064	−6593	0.6869	49	0.076
Experiment		371	0.905	0.025	−6420	0.7125	27	0.113

TABLE V. Thermodynamic derivatives of several liquid metals at the theoretical melting point (cf. Table III). The term $1/K_T$ is the bulk modulus; c_p, c_v are the specific heats; c is the velocity of sound; and α is the thermal-expansion coefficient.

Metal	$1/K_T$(kbar)	c_p(cal/mole K)	c	$10^4\alpha$ (K^{-1})	c_p/c_v
Li	96.7 (?)	8.013 (7.264)	4688	2.6 (1.6)	1.135
Na	50.6 (52.3)	7.936 (7.605)	2527 (2526)	3.0 (2.44)	1.137 (1.099)
K	23.8 (26.2)	8.057 (7.682)	1857 (1880)	3.5 (2.8)	1.151 (1.12)
Al	534 (430)	7.89 (7.58)	5062 (4720)	0.76 (1.16)	1.142 (1.25)

crudely approximated by a step function at $r=\sigma$ (or perhaps by a δ function, but the idea remains the same),

$$g_\sigma(r) \cong C\Theta(r-\sigma), \tag{25}$$

with C a constant of order unity. Small variations in σ will cause U to change as follows:

$$\delta U \cong \left(\frac{\rho}{2}\int \frac{\partial g_\sigma(r)}{\partial\sigma}\,\phi(r)\,d^3r\right)\delta\sigma$$
$$\cong -C\frac{4\pi\rho\sigma^3}{2}\,\phi(\sigma)\frac{\delta\sigma}{\sigma}. \tag{26}$$

If σ happens to fall near the zero of $\phi(r)$, then variations of σ will not cause large variations in the internal energy and latent heat. This can happen if σ is chosen fortuitously. But in general, $\phi(\sigma)$ will not be small, and indeed the calculations reported here typically give values of 2 mRy. Using nominal values of ρ and σ, we find $\delta U \cong 0.2$ mRy, or 20% of the latent heat when σ is varied by only 1%. Thus, systematic errors in σ could have easily wiped out any trend in alkali-metal latent heat.

The variational approach to the latent-heat calculation avoids this problem because σ is chosen self-consistently with the metal potential $\phi(r)$. Thus, any error made for one alkali metal will be made for all, but the trend in latent heats will not be lost.

Table IV shows the model dependence of the melting properties of sodium. The calculations are done by varying the constant a in Eq. (23), or by using a different radial distribution function. The results illustrate again the difficulty of making latent-heat calculations. Perhaps more important, the results show that it is not just the difficulty of representing a system by a hard-sphere system that leads to errors, but also the fact that the hard-sphere system *itself* is not sufficiently well characterized to allow precise latent-heat calculations. Thus, the use of a better form of thermodynamic perturbation theory will not remove the discrepancies between theory and experiment until the hard-sphere system itself is better understood. It should be emphasized that this conclusion applies only to melting properties; for ordinary predictions, the hard-sphere system's properties are sufficiently well characterized, as we will see later.

Aside from the model dependence of the calculation, a characteristic not previously discussed, the present results agree generally with previous work by Stroud and Ashcroft. Typically, $\eta \cong 0.45$ at melt and is independent of pressure. This value is larger than that of Stroud and Ashcroft, but it is very sensitive to the model, varying from 0.42 to 0.50 as the model is changed. The melting curve does not show the maximum found by Stroud and

TABLE VI. Model dependence of calulated properties for liquid solium. The CS, OZ, and V refer, respectively, to the Carnahan-Starling, Ornstein-Zernike, and Virial equations for the hard-sphere free energy A_0. The PY and VW refer, respectively, to the Percus-Yerick and Verlet-Weis approximations to the hard-sphere radial distribution function. In every case, properties are calculated at the theoretically determined melting point shown.

	Model				
	CS/VW	CS/PY	OZ/PY	V/PY	Experiment
T_M (K)	395	346	372	270	371
ρ_L (g/cm^3)	0.878	0.901	0.889	0.933	0.927
$1/K_T$ (kbar)	47.9	50.6	49.0	55.4	52.3
c_p (cal/mole-K)	7.68	7.93	7.80	8.42	7.61
C (m/sec)	2506	2527	2511	2569	2526
$10^4\alpha$ (K^{-1})	2.93	3.00	2.96	3.11	2.44
c_p/c_v	1.152	1.137	1.145	1.111	1.099

Ashcroft; however, the calculation here is done with sufficient care at high density to ensure that no spurious maximum is generated. Furthermore, the present calculation always satisfies the Clausius-Clapeyron relation.

Table V presents thermodynamic derivatives (compressibility, thermal expansion, and so on) for each of the metals concerned. In each case, the calculation is done at the predicted melt temperature and density given in Table III, rather than at the experimental values. (To do otherwise would introduce systematic errors due to the fact that the pressure would not be zero.) In general, agreement between theory and experiment is reasonably good, being worst for the thermal-expansion coefficient α and related quantities (e.g., C_p/C_v). For sodium, we calculate a value of α 23% too large, while Stroud and Ashcroft find a value 26% too small. In all cases where data exists, the differences between the alkali metals are well reproduced. The agreement between theory and experiment is not so good for aluminum as for the alkali metals, which suggests that a nonlocal pseudopotential may be required to describe aluminum.

Table VI shows the effect of model dependence on the thermodynamic derivatives of Na. In each approximation shown, the melt temperature and density are those predicted by the approximation given in the table. It will be seen that in no case is the model dependence of the thermodynamic derivatives very great.

We have carried out calculations of thermodynamic properties away from the melt line in anticipation of measurements done simultaneously at pressure and temperature.[11] Since data does not yet exist for such conditions, we present only a few of the more interesting results. Figure 6 shows the specific heat of sodium as a function of temperature alone. The agreement between theory and experiment is seen to be extremely good.[29] In particular, we reproduce the fall in specific heat to a minimum value. This fall had been attributed to a failure of the liquid to achieve complete randomness on melting. However, the theoretical model used here does not consider such structural effects in the liquid, so the agreement with experiment is surprising.

As an indication of how the theory fares at low density, Fig. 7 displays the velocity of sound of sodium over a wide range of temperature for several pressures. The agreement with experiment[30] at low temperatures (near T_m) is very good, but there is a notable discrepancy in the trends of the two (nominally) zero-pressure curves. The downward curvature of the experimental data reflects the fact that, near the critical point, the velocity of sound tends to become small. Since the theory presented here cannot be expected to apply at the critical density because of the metal-insulator transition, one is left with a small upward curvature. At the highest temperature shown in Fig. 6, the density has fallen to 0.7 of the normal liquid density. At this density, the error in the velocity of sound is still only 20%. However, it is clear that this error rapidly worsens as the critical density is approached. Some of the discrepancy is due to a bad initial slope of the veloc-

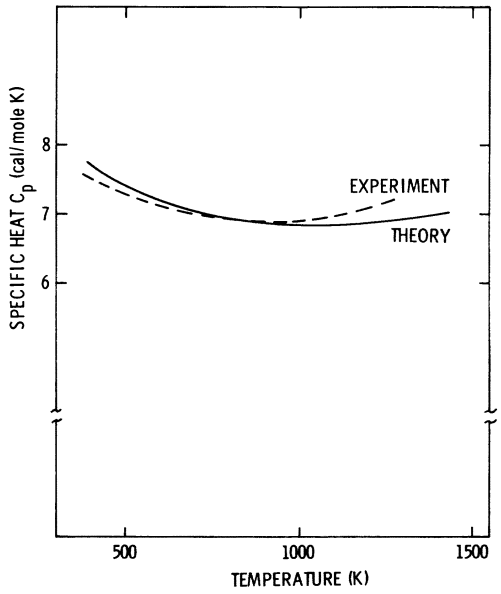

FIG. 6. Temperature dependence of the specific heat of liquid sodium.

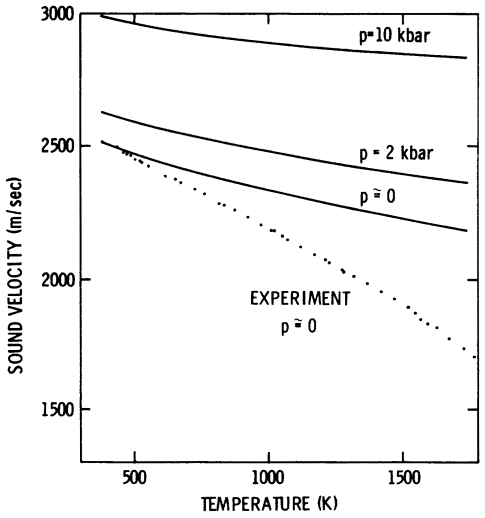

FIG. 7. Temperature dependence of the velocity of sound of liquid sodium at vapor pressure, and at elevated pressures.

ity-vs-temperature plot. This condition probably reflects small errors in the pseudopotential or problems in the use of a hard-sphere reference system. Problems associated with the metal-insulator transition itself would cause the two curves to diverge significantly only at temperatures in excess of 1600 °K. For densities below perhaps one-half of the normal liquid density (i.e., about twice the critical density) one would no longer be able to ignore the Mott transition.

As a point of reference, the Einstein temperatures calculated, respectively, for Li, Na, K at melt were 298, 121, 77 °K, versus the experimental values of 335, 156, 91 °K. This might be considered indirect evidence in support of the Einstein model as a reference system. The validity of the hard-sphere reference system for liquid alkali metals has been established by comparing the radial distribution functions.[31]

V. SUMMARY

Calculations have been presented for thermodynamic properties of several liquid metals, not only at the melting point but also over a range of temperatures and pressures. By considering several alkali metals as well as aluminum, it has been demonstrated that it is possible to predict trends in the properties of a series of metals. For latent-heat calculations, great care was required to accomplish this and to avoid getting the spurious trend seen in previous work.

The results for aluminum were not as satisfactory as those for the alkali, although still in reasonable agreement with experiment. Better agreement should be had when a nonlocal pseudopotential model is employed; such a model will also allow the study of other metals, in particular mercury, which allows easy experimental investigation.

From the predicted critical-point estimates, it was hypothesized that the theory might be carried out toward the critical point with some success. To test this, calculations were carried out to low densities and higher temperatures in an effort to locate the critical point. With reference to Fig. 5, this operation would be done by carrying out another tangent construction between the two dips in the liquid free-energy curve. Unfortunately, the theory does not predict the second dip in the curve, but rather follows the dashed line. The dip occurs because the conduction electrons can lower their energy by dropping into atomic orbitals once the density becomes low. The theory presented here cannot account for this metal-insulator transition effect.

By comparing the theory with experimental data for the velocity for sound, it was found that the metal-insulator transition could be safely ignored out to perhaps one-half the normal density. But, to get a theory which predicts a critical point, and which thereby gives reasonable thermodynamic properties in the vicinity of the critical point, will require consideration of the Mott transition.

ACKNOWLEDGMENT

The author wishes to thank W. G. Hoover and D. A. Young for a critical reading of the manuscript.

---

*This work was supported by the United States Atomic Energy Commission under Contract No. AT-(29-1)-789.

[1]H. C. Anderson, J. D. Weeks, and D. Chandler, Phys. Rev. A 4, 1597 (1971).
[2]J. A. Barker and D. Henderson, J. Chem. Phys. 47, 4714 (1967); D. Henderson and J. A. Barker, Phys. Rev. A 1, 1266 (1971).
[3]L. Verlet and J. J. Weis, Phys. Rev. A 5, 939 (1972).
[4]G. A. Mansoori and F. B. Canfield, J. Chem. Phys. 51, 4958 (1969); 51, 4967 (1969).
[5]P. Ascarelli and R. J. Harrison, Phys. Rev. Lett. 22, 385 (1969).
[6]D. Schiff, Phys. Rev. 186, 151 (1969).
[7]D. L. Price, Phys. Rev. A 4, 358 (1971).
[8]H. D. Jones, J. Chem. Phys. 55, 2640 (1971).
[9]D. Stroud and N. W. Ashcroft, Phys. Rev. B 5, 371 (1972).
[10]W. M. Hartmann, Phys. Rev. Lett. 26, 1640 (1971).
[11]H. A. Spetzler, M. D. Meyer, and H. D. Jones (unpublished).
[12]J. A. Krumhansl, in *Physics of Solids at High Pressures*, edited by C. T. Tomizuka and R. M. Emrick (Academic, New York, 1965).
[13]W. A. Harrison, *Pseudopotentials in the Theory of Metals* (Benjamin, New York, 1966).
[14]J. Rasaiah and G. Stell, Mol. Phys. 18, 249 (1970); see also Ref. 4.
[15]W. G. Hoover, S. G. Gray, and K. W. Johnson, J. Chem. Phys. 55, 1128 (1971).
[16]D. C. Wallace, Phys. Rev. 176, 832 (1968); 178, 900 (1969).
[17]D. J. W. Geldart and S. H. Vosko, Can. J. Phys. 44, 2137 (1966); 45, 2229(E) (1967).
[18]N. W. Ashcroft and D. C. Langreth, Phys. Rev. 155, 682 (1967).
[19]Most formulations of the energy do not express E as a sum of pair potentials; thus it has not been necessary to do this analysis in previous energy calculations.
[20]D. C. Wallace, Phys. Rev. 187, 991 (1969).
[21]T. R. Koehler, N. S. Gillis, and D. C. Wallace, Phys. Rev. B 1, 4521 (1970).

[22]A. V. Grosse, J. Inorg, Nucl. Chem. 22, 23 (1961); 24, 147 (1962).
[23]L. Verlet and D. Levesque, Physica 36, 245 (1967).
[24]For this computation, σ is determined by the condition $\phi(\sigma)=0$, and since the value of σ that results is only weakly density dependent, a density one-fifth of the normal density ρ_N is arbitrarily chosen as an estimate of the critical density ρ_C. Equation (16) then gives a value of ρ_C (Table II) (which is generally different from the starting value of $\frac{1}{5}\rho_N$). For the critical temperature determination, the experimental critical density is used in setting the well depth.
[25]A. A. Maradudin, E. W. Montroll, and G. H. Weiss, in *Solid State Physics*, 2nd ed., edited by F. Seitz, D. Turnbull, and H. Ehrenreich (Academic, New York, 1971), Vol. 3.
[26]K. Fuchs, Proc. R. Soc. Lond. A 151, 585 (1935).
[27]N. F. Carnahan and K. E. Starling, J. Chem. Phys. 51, 635 (1969).
[28]P. E. Choquard, *The Anharmonic Crystal* (Benjamin, New York, 1967).
[29]D. C. Ginnings, T. B. Defoe, and A. F. Ball, J. Res. Natl. Bur. Stand. 45, 23 (1950).
[30]M. G. Chasanov, L. Leibowitz, D. F. Fisher and R. A. Blomquist, J. Appl. Phys. 43, 748 (1972); L. Leibowitz, M. G. Chasanov, and R. A. Blomquist, J. Appl. Phys. 42, 2135 (1971).
[31]A. J. Greenfield, J. Wellendorf, and N. Wiser, Phys. Rev. A 4, 1607 (1971).